Organic Process Research & Development **2009,** *13,* 1276–1283

A Novel Crystallization Methodology To Ensure Isolation of the Most Stable Crystal Form

Aaron Cote,* George Zhou, and Mary Stanik

Global Pharmaceutical Commercialization, P.O. Box 2000, Merck & Co., Rahway, New Jersey 07065, U.S.A.

Abstract:

It is critical to consistently achieve the desired crystal form for an active pharmaceutical ingredient (API) because crystal form may affect the compound's chemical stability, bioavailability, and pharmaceutical processing performance. The extent to which a crystallizing system is driven by growth vs nucleation is dependent upon the level of supersaturation, defined as the difference between solution concentration and solubility. We describe a method for the accurate measurement of real-time supersaturation, which enabled us to develop and optimize an API crystallization via a feedback-control loop based on concentration measurement with online FTIR. In this contribution we discuss a novel extension of the published work [Zhou, G. X.; et al. ***Cryst. Growth Des.*** **2006,** ***6,*** **892−898] which ensured robust isolation of the thermodynamically most stable crystal form of an API. The system of interest is a monotropic polymorphic system with overlapping metastable zones. In order to ensure exclusive isolation of the desired form within a reasonable cycle time, a three-pronged approach was applied—maximize seed surface area through the use of milled seed, run the crystallization at a high temperature to increase crystal growth rate, and perform the crystallization at a high level of supersaturation relative to the desired, more stable form while keeping the concentration below the equilibrium solubility of the less stable polymorph. By carefully selecting the seed loading, we were also able to dial-in the target particle size directly via a growth-dominated crystallization, thus eliminating the need for post-crystallization product milling. As a result, a robust, efficient, and reliable crystallization process has been achieved to ensure isolation of the desired polymorph at target particle size.**

Introduction

The majority of active pharmaceutical ingredients (API) exhibit polymorphism, and it is critical to consistently achieve the desired polymorph for these API because crystal form may affect the chemical stability, bioavailability, and pharmaceutical processing performance. With very few exceptions, the thermodynamically most stable form is the one pursued for large-scale production. Therefore, the development of a crystallization step capable of ensuring the consistent isolation of the most stable crystal form is often a critical part of the process development effort. Because this is such a commonly encountered problem, establishing a "best practice" approach with universal applicability would be of great value to the field of pharmaceutical crystallization. In this contribution, just such a technique is described, and its application to a particularly challenging polymorph crystallization problem is elaborated.

When anhydrous polymorphs exist, the relative stability of the various forms may be assessed by measuring the solubility of each form in the same solvent at the same temperature. The most stable crystal form at a particular temperature is the form with the lowest solubility at that temperature, and progressively less stable forms will have progressively higher solubility. In order to crystallize from solution, one must create a solution concentration in excess of the solubility, a condition referred to as supersaturation. In the absence of supersaturation, crystallization will not occur. Therefore, the most effective way to ensure that a metastable polymorph will not nucleate out of solution is to maintain the solution concentration *below* the solubility of that particular form. Central to the strategy discussed herein is the recognition that different polymorphs have different solubilities and, therefore, there is a window in the operating space that affords the necessary supersaturation with respect to the most stable polymorph while avoiding supersaturation with respect to the next most stable form. That window is simply the region that lies in between the solubility curves of these two forms. Thus, as a general rule, if one wishes to crystallize the most stable form exclusively, one may do so by navigating the solution-phase concentration between these solubility curves throughout the course of the crystallization. If the forms in question are enantiotropic rather than monotropic, one must identify the transition temperature, decide which form will be targeted, and then conduct the crystallization exclusively on the side of the transition temperature which favors the target form as the thermodynamically most stable (i.e., least soluble).

The concept of operating between the solubility curves of the more and less thermodynamically stable crystal forms of an API has been demonstrated previously by colleagues at Merck.[1] In that citation, the authors selected a solvent composition which maximized the growth rate of the desired more stable Form I, seeded heavily with Form I with the system supersaturated with respect to Form I but below the solubility of the undesired Form II, and applied an antisolvent addition profile that maintained the solution-phase concentration below the Form II solubility. This approach allowed the authors to selectively isolate the desired Form I product. The current work advances this methodology by replacing the trial-and-error approach to selecting the antisolvent addition rate with a feedback-controlled approach that allows an optimal batch recipe to be derived more efficiently and elegantly.

* To whom correspondence should be addressed. E-mail: aaron_cote@merck.com.

(1) Wang, J.; Loose, C.; Baxter, J.; Cai, D.; Wany, Y.; Tom, J.; Lepore, J. *J. Cryst. Growth* **2005**, *283*, 469–478.

10.1021/op900095n CCC: $40.75
Published on Web 10/01/2009

In the specific case study presented herein, a drug candidate (referred to as MK-A) was shown to exhibit polymorphism, with two anhydrous forms, Forms I and II, relevant to the discussion. Early development work was done with Form I, as Form II had not been identified at that time. It was determined that Form I required particle size reduction to achieve the desired bioavailability. During jet milling (a.k.a., air attrition milling), Form I underwent a detectable amount of form conversion to Form II, which was subsequently determined by way of solubility vs temperature measurements to be the more stable form across the temperature range of interest.

Although Form I was the less thermodynamically stable of the forms, it was readily isolated because it was highly kinetically favored. In fact, during early process development, pure Form II was never crystallized directly from solution, as all attempts to do so (from a variety of solvents under a variety of operating conditions), yielded a mixture of Forms I and II. The isolation of Form II samples devoid of detectable amounts of Form I was achieved only through long-duration, high-temperature slurry turnover experiments or through prolonged exposure of the API to mechanical stress as achieved during ball milling.

An initial multi-kilogram delivery of Form II was made by slurrying Form I in toluene at 80 °C (Form I solubility = 35 mg/mL; Form II solubility = 20 mg/mL) with Form II seed for more than 30 h. While the desired Form II was ultimately isolated, purity was compromised due to product degradation at this high temperature. Furthermore, because particle size control was critical to achieving target bioavailability with Form II, post-crystallization milling of this sample was required. Jet milling of Form II proved problematic, as the impinging crystals abraded the metal raceway, resulting in a product with an unacceptably high level of heavy metals. Pin milling of Form II proved less problematic, and the pin milled product (average particle size ~10 μm vs ~4 μm from jet milling) gave an acceptable dissolution profile and associated *in vivo* performance.

While the pin milled product from the slurry turnover process satisfied the short-term need, the long-term goal was to develop a process to isolate Form II directly via a crystallization (ideally as part of the final reaction step) with a time cycle of less than 24 h while avoiding the formation of any new impurities. Additionally, the high cost and industrial hygiene issues associated with the API pin milling step provided motivation for controlling the particle size distribution (PSD) directly via the final crystallization.

After a number of crystallization experiments using different solvent systems, seed loadings, and crystallization times failed to achieve the necessary crystal form control, it became clear that a more rigorous, rational approach was required. Online monitoring with focused beam reflectance measurement (FBRM), Fourier transform infrared spectroscopy (FTIR), and Raman spectroscopy revealed that the crystallization kinetics were very slow and that, when the system accumulated supersaturation, nucleation of the higher free energy Form I was observed. At no point during the development of this compound was primary nucleation of Form II from solution observed. In order to avoid nucleation of Form I, it was critical to control the solution concentration of the API below the Form I solubility as described above. The challenge was to do this while satisfying the design criteria with respect to cycle time and PSD specifications.

In order to accomplish these goals, the following combination of best practices was applied:

1. Utilize a very large amount of Form II seed surface area, recognizing that the rate of supersaturation relief via Form II crystal growth (i.e., the Form II mass deposition rate) is directly proportional to the available seed surface area (see eq 6.18 of Mullin's text[2]). This was accomplished by seeding with small seed (average size ~2 um, surface area ~12 m^2/g) generated via slurry media milling and by using relatively large seed loading.[3] Ultimately 10 wt % seed loading was utilized, as this gave acceptable time cycle and allowed the final product particle size to be dialed-in to the target size.

2. Run the crystallization at elevated temperature to increase the Form II growth rate.

3. Control the antisolvent addition and batch cooldown rates to maintain a high level of supersaturation with respect to Form II without exceeding the solubility of Form I.

It is the last of these three elements that was challenging and contributed to the novelty of this strategy. Fortunately, with the recent advances in process analytical technology (PAT) and automation of batch crystallizers, batch crystallization processes can be designed to follow a predefined supersaturation profile by feedback control.[4] As early as 2002 Togkalidou et al. reported measuring solute concentration with online FTIR for crystallization processes via cooling or antisolvent addition.[5] Since then, many researchers such as Wang,[1] Zhou,[6] Woo,[7] Liotta,[8] and Kee[9] have reported their work with online FTIR measurement of solute concentration in the crystallization processes. Crystallization via feedback control has also been reported in the recent years.[6–13] Feedback-control crystallization via online FTIR measurement was evaluated and implemented in this study. Herein we also describe a new approach for automated and accurate measurement of solubility by implementing a temperature loop that helps to accelerate the approach to equilibrium. In addition, this contribution illustrates the

(2) Mullin, J. W. *Crystallization*, 4th ed.; Butterworth-Heinemann: Oxford, 2001.
(3) Johnson, B. K.; Tung, H.-H.; Lee, I.; Cote, A. S.; Starbuck, C. , Midler, M. Processes and Apparatuses for the Production of Crystalline Organic Microparticle Compositions by Micro-Milling and Crystallization on Micro-Seed and Their Use, U.S. Patent Application 20090087492, 2009.
(4) Fujiwara, M.; Nagy, Z. K.; Chew, J. W.; Braatz, R. D. *J. Process Control* **2005**, *15*, 493–504.
(5) Togkalidou, T.; Tung, H.-H.; Sun, Y.; Andrews, A.; Braatz, R. D. *Org. Process Res. Dev.* **2002**, *6*, 317–322.
(6) Zhou, G. X.; Fujiwara, M.; Woo, X. Y.; Rusli, E.; Tung, H.; Starbuck, C.; Davidson, O. A.; Ge, Z.; Braatz, R. D. *Cryst. Growth Des.* **2006**, *6*, 892–898.
(7) Woo, X. Y.; Nagy, Z. K.; Tan, R. B. H.; Braatz, R. D. *Cryst. Growth Des.* **2009**, *9*, 182–191.
(8) Liotta, V.; Sabesan, V. *Org. Process Res. Dev.* **2004**, *8*, 488–494.
(9) Kee, N. C. S.; Tan, R. B. H.; Braatz, R. D. *Cryst. Growth Des.* **2009**, *9*, 3044–3051.
(10) Fujiwara, M.; Chow, P. S.; Ma, D. L.; Braatz, R. D. *Cryst. Growth Des.* **2002**, *2*, 363–370.
(11) Gron, H.; Borissova, A.; Roberts, K. J. *Ind. Eng. Chem. Res.* **2003**, *42*, 198–206.
(12) Yu, Z. Q.; Chow, P. S.; Tan, R. B. H. *Ind. Eng. Chem. Res.* **2006**, *45*, 438–444.
(13) Lindenberg, C.; Krattli, M.; Cornel, J.; Mazzotti, M. *Cryst. Growth Des.* **2009**, *9*, 1124–1136.

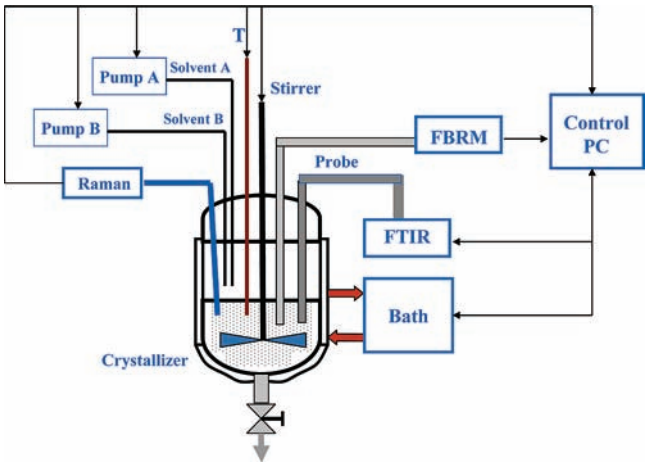

Figure 1. **Schematic of apparatus and instrument setup.**

approach that constructs robust calibration models for a complicated solution matrix that is the product of a reaction.

Experimental Section

Experimental Setup. The crystallizer (Figure 1) used in this study was interfaced with three online analyzers: FTIR, FBRM, and Raman spectroscopy. The FTIR with a diamond ATR probe (ReactIR 4000 by Mettler-Toledo) was used to measure the liquid-phase concentration of the solute. The instrument was calibrated by using chemometric techniques[5−7] to correlate the IR spectra to the corresponding solvent compositions and solute concentrations at which they were collected. Lasentec FBRM (Mettler-Toledo) was employed to measure the particle size distribution profiles or check for the presence of crystals during the process. A Raman spectrometer (Kaiser Optics, Inc.) was used to determine the crystal form(s) of the solid phase present in the crystallizer. The crystallizer was a 500 mL jacketed glass vessel equipped with overhead mechanical stirrer and a custom head designed to accommodate the many probes and reagent charge lines. The temperature was controlled by a water bath (Haake F8), and solvents were delivered by programmable syringe pumps (Harvard Apparatus PHD 4400). The control PC received signals from the thermocouple, FTIR, FBRM, and Raman spectroscopy and was used to control the charge pumps and water bath. The crystallization procedures were enabled on a graphical user interface written in Microsoft Visual Basic 6.0 for the automatic data collection, solubility measurement, and concentration control. The Visual Basic interface called a program written in MATLAB for calibration model development using chemometrics, namely, partial least-squares (PLS) regression methods.[14]

Isolated solids were analyzed by X-ray diffraction (Phillips Analytical X'pert Pro X-ray powder diffraction) to check crystal form while particle size distribution (PSD) was measured using light scattering (Microtrac SRA-150).

Materials. The API referred to as "MK-A" is an HIV integrase candidate made in-house at Merck & Co., Inc. This crystallization process follows immediately after a quenching reaction in which sodium ethoxide is quenched with acetic acid to give a solution (referred to as solvent A) of API in ethanol with sodium acetate and excess acetic acid. To develop the crystallization process, a simulated end-of-reaction solution was prepared directly with API (Form I or Form II), ethanol (HPLC grade from Aldrich), acetic acid, and sodium acetate (both ACS grade from Aldrich). It was important to use this simulated end-of-reaction stream during both the construction of the calibration model and the solubility measurement, rather than simply using pure ethanol. Not only does the presence of sodium acetate and acetic acid affect the solubility of the API, but these species affect the IR spectra significantly and must be properly accounted for during the PLS model development. Failure to use this relevant media would have compromised the utility of this control scheme. During the crystallization, HPLC grade water (from Aldrich) was added as the antisolvent (referred to as solvent B). Media milled Form II seed crystals (particle size: ~2 um) were used for the controlled crystallization studies. This seed was generated in and charged as a 10 wt % slurry in 60/40 v/v water/ethanol.

Automated Calibration. To streamline the collection of IR spectra, addition of solvent, and measurement of concentration, an automated operation protocol has been developed. During the calibration, this procedure calculates the concentration and solvent composition based on the amount of solute and solvents that have been charged to the crystallizer, thus avoiding the uncertainties associated with sampling for off-line analysis via chromatographic methods. The off-line technique is particularly challenging when sampling a hot solution due to the potential for the solute to crystallize out during the sample preparation. Typically, the calibration procedure is performed according to the following recipe. API plus a specific amount of solvent A is added to create a clear solution of known composition. Solvent B (antisolvent) is then added while IR data is collected until FBRM detects the presence of particles. This marks the metastable limit. Solvent A is then added again until the solute dissolves, and the procedure is repeated, stepping down progressively to a more dilute system. By sequentially adding the antisolvent and solvent to the crystallizer according to this procedure, IR spectra of clear solutions with specific known solute concentrations and solvent/antisolvent ratios are collected automatically. Normally the metastable zone can be detected by FBRM when continuously adding antisolvent. In this case, the metastable zone width was so large that Form II nucleation was never observed. Therefore, a modified approach was applied in which the metastable limit detection was turned off and prescribed amounts of solvents B and A were charged during each cycle. This process is presented pictorially in Figure 2. It should be noted that it is generally advantageous to have a rough estimate of the solubility at the extremes of the solvent composition range of interest so that the calibration model can be created for the relevant operating space.

Once representative spectra across a wide range of solute concentrations and solvent compositions were obtained, a reliable calibration model was built automatically with the partial least-squares regression in MATLAB. For the solubility of MK-A in the mixture of ethanol, acetic acid, sodium acetate, and water, an optimum PLS model with 5 factors was built in the spectral region 1800−1000 cm^{-1} with a standard error of cross validation (SECV) of 0.51 mg/mL across the concentration

(14) Beebe, K. H.; Kowalski, B. R. *Anal. Chem.* **1987**, *59*, 1007A–1017A.

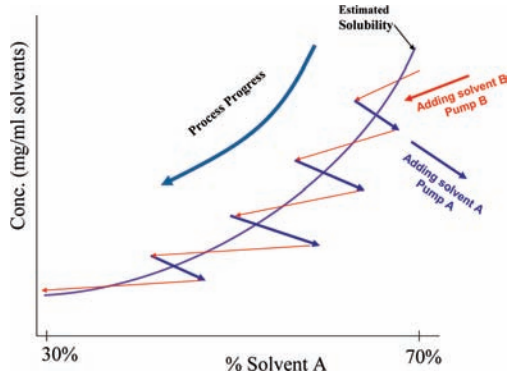

Figure 2. **Diagram of automatic calibration procedure for antisolvent B (water) addition to solvent A (ethanol, acetic acid, sodium acetate) at constant temperature of 65 °C.**

range of 0−200 mg/mL and solvent composition range of 30−70 vol % A (ethanol/(ethanol + water)).

Solubility Measurement. Solubility is obtained through a program that automatically collects IR spectra for slurries at different solvent compositions. In general, the process works as follows. The batch starts with a slurry of solute in solvent A; solvent B is added incrementally to the vessel, with the batch aged at each stage for a sufficient time to allow the liquid and solid phases to reach equilibrium, as determined by a leveling off in the measured liquid-phase concentration. At the end of each stage, the system automatically collects and saves five spectra. The process is repeated until spectra are collected for six stages with different levels of solvent A spanning the range of interest.

Typically, a 6-point solubility curve can be generated in less than 24 h (for both calibration and solubility measurements). However, in this case, the crystallization kinetics were so slow that it would have taken many days to generate each curve if the system were allowed to equilibrate at each point by releasing supersaturation through crystallization. In order to automate this procedure such that each solubility curve could be generated within 24 h, a modified approach was applied. Specifically, after each antisolvent addition step, the batch was cooled by 20 °C in order to increase supersaturation and promote more rapid crystallization (Figure 3). The batch was subsequently reheated to dissolve the material that had crystallized in excess of what would be in equilibrium at the target measurement temperature (65 °C in this case). This approach took advantage of the fact that the dissolution rate was much faster than the crystallization rate. After each batch reheat, the slurry was aged until the solution concentration leveled off and remained constant for 15 min, then the IR spectra were collected to measure the steady-state solution concentration. Because there was a risk of crystallizing out the wrong form during the cooldown, Raman spectroscopy was applied to confirm that the solution at 65 °C was in equilibrium with a solid phase that was exclusively the polymorph of interest for that particular measurement. This process was performed for both Forms I and II. At the end of each solubility experiment, the solids were isolated, and crystal form was confirmed by X-ray diffraction (XRD). From the FTIR spectra, the solubility profiles were generated automatically by using the calibration model. The resulting solubility curves are illustrated in Figure 4.

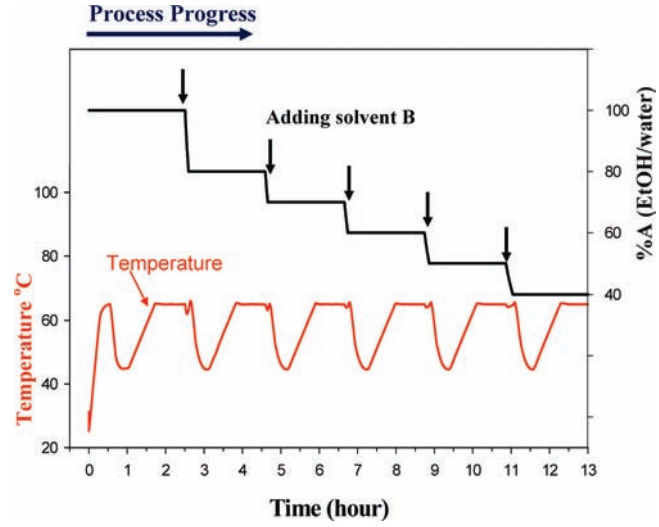

Figure 3. **Progress diagram for the automated collection of slurry spectra for solubility versus solvent composition.**

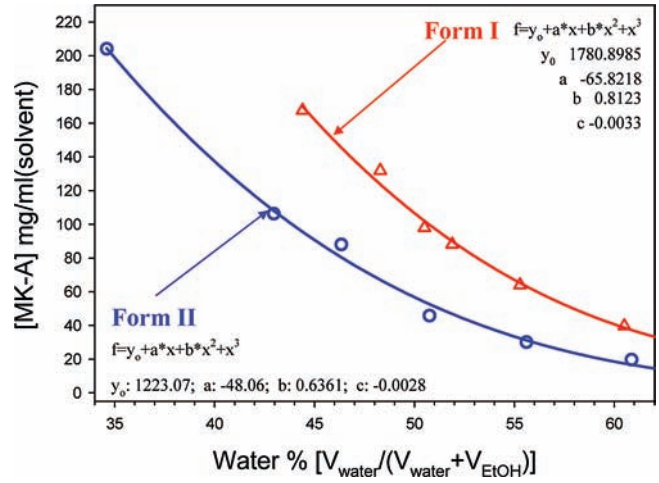

Figure 4. **Solubility curves of Forms I and II of MK-A in solvent mixture A (ethanol, acetic acid, sodium acetate) and antisolvent B (water) at 65 °C.**

In this case, the kinetics of phase change from Form I to the more stable Form II were very slow such that no form conversion was detected during the process of mapping the Form I solubility. It is precisely because these kinetics were so slow that application of this feedback-controlled approach was required to achieve isolation of Form II. Had the rate of form conversion been more rapid such that appreciable conversion to Form II occurred during the time required for the system to equilibrate at the Form I solubility concentration, then this solubility mapping technique would not have been viable. However, if the rate of form conversion were so rapid, it is likely that less sophisticated processing approaches could have achieved the goal of Form II isolation.

Results and Discussion

At the beginning of the process development effort, it had not been determined whether an "antisolvent followed by cooldown" or "cooldown followed by antisolvent" approach would be the more effective route toward the final isolation conditions. Therefore, the calibration and solubility measurement process was also performed as a function of temperature

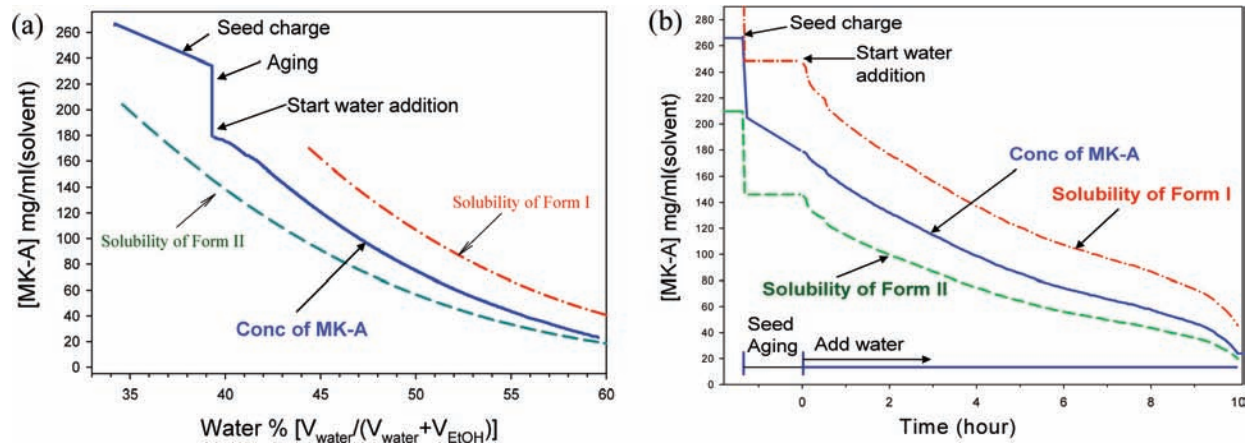

Figure 5. **Solubility curve and crystallization profiles at 65 °C for MK-A feedback-controlled addition applied to maintain 33% supersaturation: (a) vs % water and (b) vs time.**

at the seed point solvent composition in the event that a "cooldown first" process was selected. During the development, it was discovered that the Form II growth kinetics were a stronger function of temperature than of solvent composition. Because the goal was to perform the crystallization under conditions that favored high Form II growth rate, operating at high temperature for the bulk of the crystallization was demonstrated to be the most advantageous strategy. Therefore, work was focused on the high-temperature antisolvent process, and work done on the "cooldown first" process is not presented here.

Fortunately, in the case of the antisolvent addition process, the operating window (defined as the region between the two solubility curves in Figure 4) is relatively large, as the ratio of Form I solubility to Form II solubility is 1.7 ± 0.1 across the solvent composition range of interest. The implication is that exclusive Form II crystallization can be achieved with a rather substantial driving force of approximately 70% supersaturation. This made the approach very attractive.

Crystallization via Feedback Control. In order to minimize nucleation and promote crystal growth, small media milled seed with average particle size of ~2 μm and surface area of ~12 m^2/g was utilized during the feedback-controlled crystallization studies. The choice of this high surface area seed was a critical element of the successful final process. Different amounts of seed loading were evaluated with respect to their ability to facilitate an "all growth" crystallization process (as monitored by FBRM) while achieving the target average particle size for the isolated product (target: 8−15 μm). Using abundant seed surface area (10% seed loading) and operating at 65 °C, one can achieve these two goals while limiting batch cycle time to less than 24 h.

Figures 5−9 present the output for a 27-g feedback-controlled run performed with 33% Form II supersaturation maintained throughout the antisolvent addition. For this run, MK-A was slurried in a solution composed of ethanol, acetic acid, sodium acetate, and water, with the water composition at 34.3 vol % (water/(water + ethanol)). The batch was heated to 70 °C to dissolve the API and then cooled to 65 °C to create supersaturation. Ten percent milled seed of Form II was charged to the crystallizer as a 10 wt % slurry in 60/40 v/v water/ethanol. This charge diluted the batch but increased the batch water composition to 39.3%, resulting in a net increase in the supersaturation. After aging for approximately 1 h, the supersaturation was relieved from 60% to 22% as the liquid-phase concentration dropped from 235 mg/mL to 178 mg/mL.

Antisolvent addition was then initiated, and water was added continuously based on the feedback-control loop. The control system calculated the instantaneous supersaturation values by subtracting the previously measured solubility concentration at the specific known solvent composition from the in-line solution concentration measurement made via FTIR. The controller then adjusted the water charge rate in order to maintain the target supersaturation. In order to navigate between the solubility curves of Form I and II in a fairly conservative manner, a relative supersaturation of 33% Form II was applied. Figure 5 presents the concentration and solvent composition profiles during the course of this antisolvent addition, showing clearly that the batch concentration stayed safely below the Form I solubility curve.

Following completion of the antisolvent charge, the batch was cooled linearly to room temperature over 7 h. This cooldown was not controlled by the feedback-control loop because more than 80% of the batch was out of solution by the time cooling was initiated, so the risk of nucleating the wrong form was considered to be low.

The FBRM profiles at this level of supersaturation are shown in Figure 6. Over the course of the antisolvent addition, the total number of counts decreased from 55,000 to 42,000 due to dilution as the batch volume increased from 150 to 211 mL. A balance on the total particles indicates that the net increase in particle count from seed introduction to product isolation was <10%, which indicates that minimal secondary nucleation occurred during the crystallization. Furthermore, the counts in the 1−5 μm channel decreased while the counts in the 28−89 μm channel increased by a comparable amount indicating that the small seeds grew as water was added. PSD analysis by Microtrac particle size analyzer indicated an average particle size of 12.2 μm, which met the target specification. A scanning electron microscope (SEM) image of the final crystallized slurry is provided in Figure 7.

Most important is the fact that this process yielded exclusively Form II, without detectable Form I present at any time during the crystallization, as monitored by Raman spectroscopy.

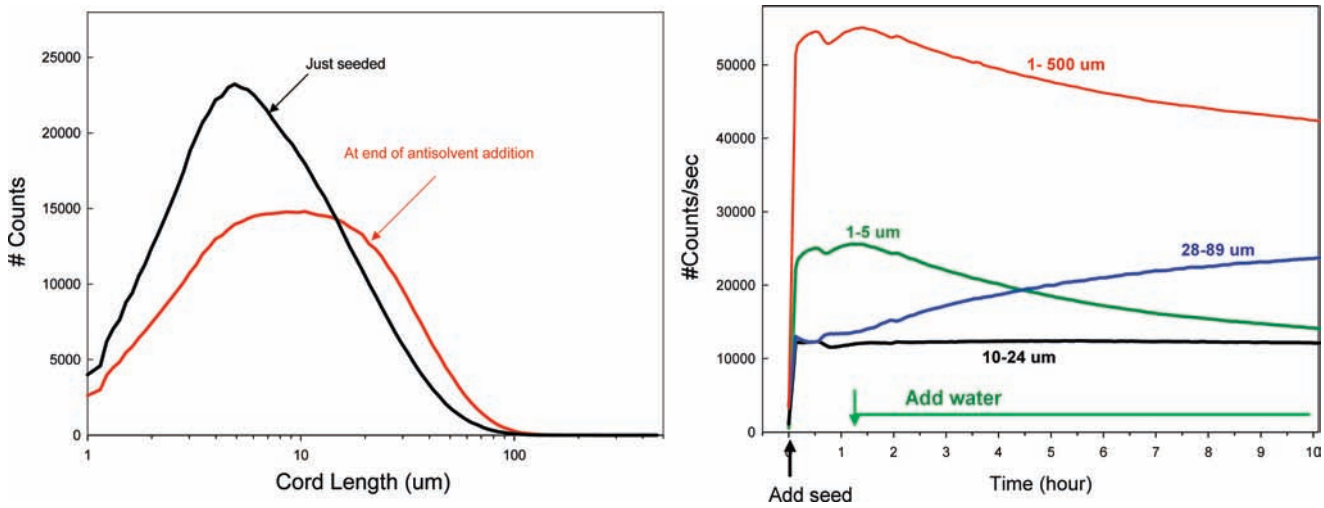

Figure 6. **FBRM PSD and size profiles for the feedback-controlled crystallization.**

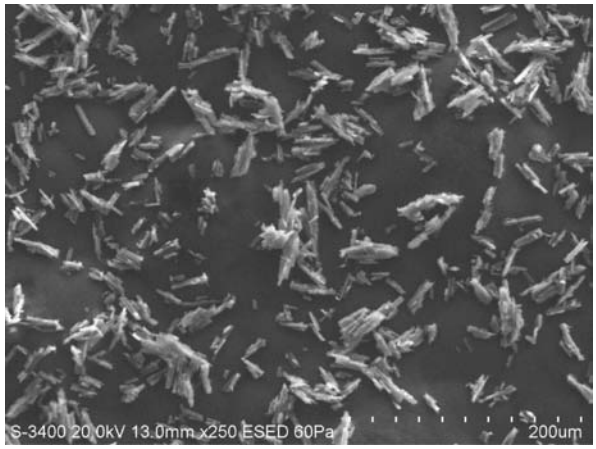

Figure 7. **SEM image of final product from the feedback-controlled crystallization.**

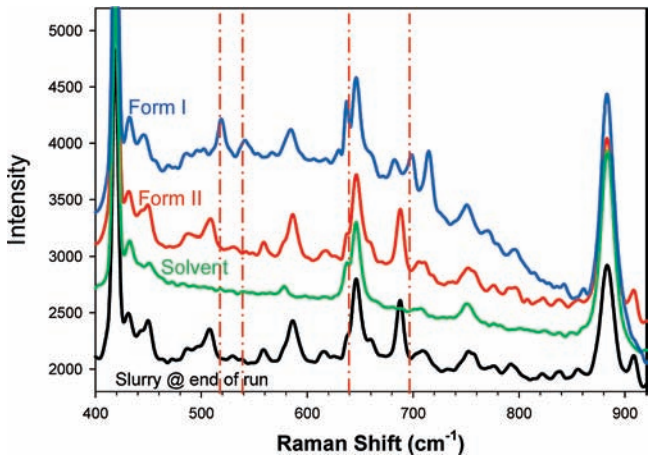

Figure 8. **Raman spectra of Form I, Form II, and the final crystallized batch from the feedback-controlled crystallization.**

A Raman spectrum taken at the end of the run is presented in Figure 8. Clearly, the spectrum of the crystallized slurry matches the Form II reference, whereas the Form I characteristic peaks at 518, 540, 637, and 700 cm^{-1} are not present at detectable levels. Typically, Raman spectroscopy has a detection limit on the order of 2−5%.[15] The absence of Form I was subsequently confirmed by XRD on the final isolated product.

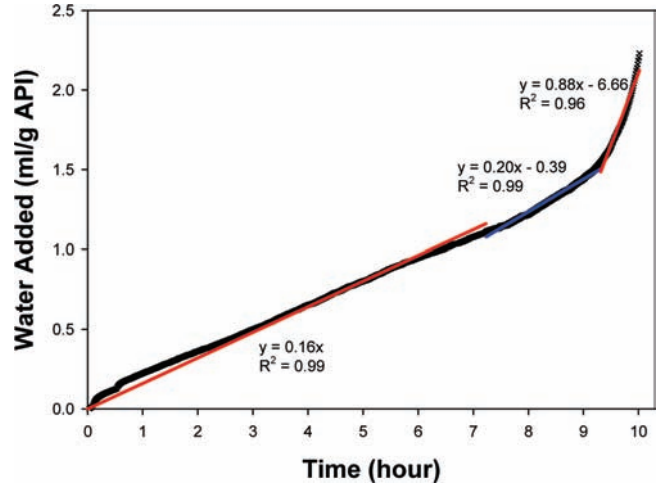

Figure 9. **Water addition profile for feedback-control run with 33% supersaturation.**

Demonstrations of the Developed Process. The feedback-control run described above achieved the polymorph control and PSD control objectives within the cycle time target, so moving forward, the plan was to use this antisolvent addition rate for larger-scale runs. The water addition profile for this run is presented in Figure 9. This curve was discretized into three linear segments in order to generate a water addition recipe for future runs so as to obviate the need for feedback control at large-scale operation. Specifically, on a 1 g of API basis, the profile derived for this run was to charge 0.16 mL/h for the first 1.11 mL of water, 0.20 mL/h for the next 0.41 mL of water, and 0.88 mL/h for the final 0.71 mL of water. Following this recipe, the total water addition time was approximately 10 h. With a 1-h seed age and 7-h cooldown, the total crystallization cycle time would be 18 h.

This three-stage water addition rate was first applied on a 6-g scale for two runs using a real reaction stream. The runs were performed with different agitator tip speeds, 0.3 and 1.7 m/s, in order to evaluate the sensitivity of the process to shear (which could promote secondary nucleation/particle breakage)

(15) Starbuck, C.; Spartalis, A.; Wai, L.; Wang, J.; Fernandez, P.; Lindemann, C. M.; Zhou, G. X.; Ge, Z. *Cryst. Growth Des.* **2002**, *2*, 515–522.

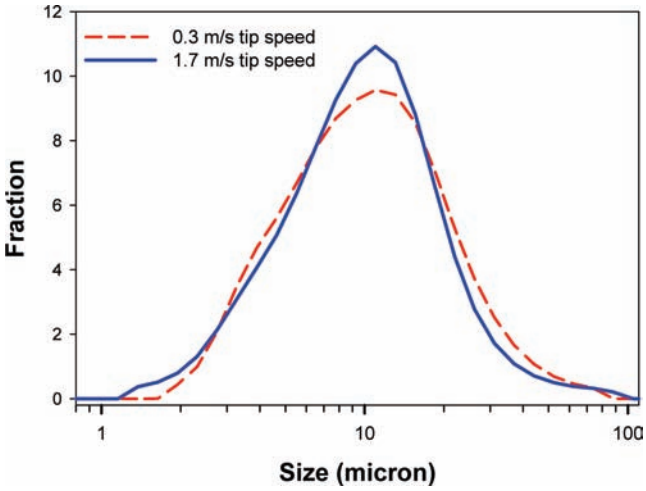

Figure 10. **PSD of 6-g runs performed with agitator tip speeds of 1.7 and 0.3 m/s.**

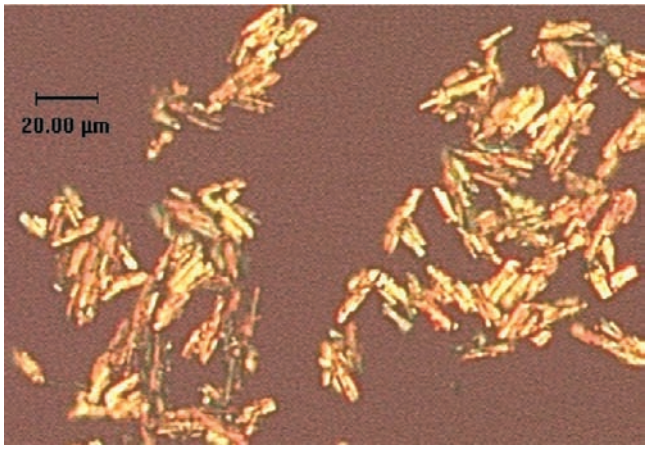

Figure 11. **Micrograph of final slurry from 6-g run performed with agitator tip speed of 1.7 m/s.**

and poor micromixing, in anticipation of potential scale-up issues. As seen in Figure 10, these runs performed similarly with respect to the particle size distributions that they produced. For the lower-shear run, in which the particles were barely suspended, the average particle size was 11.8 μm with a standard deviation of 7.0 μm and 95% < 29.2 μm, while the higher-shear run yielded an average particle size of 11.2 μm with a standard deviation of 6.1 μm and 95% < 26.0 μm. A micrograph from the higher-shear run is provided in Figure 11. Both runs yielded exclusively the desired Form II as determined by XRD analysis of the final isolated product.

Following a successful run at 36-g scale, the process was demonstrated at 10-kg scale according to the water addition recipe derived from the 33% supersaturation feedback-control run. The 10-kg run also performed as expected, yielding a purely Form II product with an average particle size of 11.9 um and a unimodal PSD.

A summary of the results across scales is presented in Table 1. In all cases, the process yielded the desired Form II with Form I levels below the detection limit of XRD. The data in Table 1 is indicative of a robust, scalable process. The particle size distributions were very similar across scales, with all runs generating an average particle size of ~12 μm, meeting the 8−15 μm target.

Table 1. **Summary of results for controlled crystallization runs**

scale of run	average particle size(μm)	standard deviation (μm)	95% < (μm)	crystal form
6 g (0.3 m/s tip speed)	11.8	7.0	29.2	II
6 g (1.7 m/s tip speed)	11.2	6.1	26.0	II
27 g (feedback controlled)	12.2	6.7	28.8	II
10 kg	11.9	5.3	26.2	II

It is worth noting that for the 10-kg batch the antisolvent addition was simply made above surface to an area of relatively poor mixing. Normally one would be concerned that poor micro-mixing could lead to high levels of supersaturation local to the antisolvent addition point which could result in nucleation of the less stable polymorph and its eventual isolation with the final product. As demonstrated both in the low-agitation 6-g run and the 10-kg run, the approach discussed in this case study is highly tolerant of poor micro-mixing, so this risk was effectively mitigated. Even if the less stable polymorph were to nucleate in a region of locally high supersaturation, it would be subsequently dissolved in the bulk fluid which is being maintained in a subsaturated state relative to that form's solubility.

In this case, the solubility curves of the two crystal forms differed considerably, so navigating between them was relatively straightforward. Had the difference in solubilities been significantly less, the need for very accurate measurement and control would have been accentuated. It is important to note that the procedure described herein ensures that the most stable crystal form will be crystallized exclusively, but it does not guarantee that this can be accomplished in a reasonable amount of time, as that depends on both the crystallization kinetics and the difference in solubility between the relevant polymorphs. Operating between two scarcely separated solubility curves would imply operating under very low levels of supersaturation, likely leading to a slow growth rate and long crystallization time. In extreme cases, this may simply be impractical from a cycle-time perspective. While one might be tempted to apply higher supersaturation in an attempt to increase growth rate and shorten cycle time, as soon as one pushes the concentration beyond the solubility of the less stable form, the guarantee of isolating the most stable polymorph is forfeited. That said, an alternative approach in which one applies feedback control to maintain the liquid phase concentration below the metastable zone limit of the unwanted crystal form in order to isolate the desired form may also warrant evaluation. Recently, Braatz and co-workers have demonstrated this approach to achieve selective isolation of the desired metastable α-form of L-glutamic acid.[9]

It is also important to note that this technique can be used as a process control tool or as a process development tool. As shown in this report, it is often not necessary for one to actually apply the feedback-control mechanism for each batch, though there is certainly no harm in doing so. In many cases, application of the recipe derived from a successful run may be sufficient to ensure success in subsequent runs. Removing the need for feedback control on each batch may provide a portability advantage by facilitating the transition of the process to facilities where the PAT tools and control systems are not integrated into the existing infrastructure. The key is to recognize when simple application of the recipe will suffice, and the basic

requirement is that the system thermodynamics (specifically, solubility) and kinetics must be relatively constant from batch to batch and across scales. For a secondary nucleation-dominated process, one would anticipate sensitivity to factors such as system shear that can change significantly upon scale-up. In cases of this sort, there may be a need to apply the feedback-control approach at the larger scale, at least once, in order to develop a recipe that is appropriate for the crystallization rate prevailing at that scale. Similarly, in cases where variability in the impurity load of the feed stream results in appreciable differences in the growth and/or nucleation rates from batch to batch, one may be compelled to use the tool for process control in order to ensure proper navigation between the curves. The problem becomes even more complicated if batch-to-batch variability in purity significantly affects the system's solubility, since the objective of this technique is to navigate between two solubility curves which are assumed to be fixed. Clearly, the situation can become complicated if the kinetics and/or thermodynamics change from batch to batch, but in the example presented herein, the tool provided an elegant solution to a very challenging problem.

Conclusions

A methodology for controlling and optimizing robust crystallization processes that are capable of consistently delivering the most stable crystal form has been presented, along with details regarding the application of this technology to a challenging example. The approach is based on the accurate measurement and closed-loop control of supersaturation during batch cooling or antisolvent addition. In order to accomplish the goal of isolating the most stable polymorph exclusively, solubility curves for the two most stable polymorphs are generated by applying an automated procedure enabled by PAT tools. In this case, generating accurate solubility data utilizing our standard automated practice was not possible due to the very slow growth kinetics, so a modified approach was successfully applied. In order to ensure isolation of the desired form within an acceptable cycle time, a three-pronged approach was successfully applied: maximize seed surface area through the use of media milled seed, run the crystallization at a high temperature to increase crystal growth rate, and utilize the feedback-control approach to perform the crystallization at a high level of Form II supersaturation while keeping the concentration below the solubility curve of the less stable Form I. By properly selecting the seed loading, PSD was controlled directly, thus eliminating the need for post-crystallization product milling. As a result, a robust, scalable, and reliable crystallization process has been achieved to ensure isolation of the desired polymorph at target particle size. While the level of control afforded by this methodology may have its greatest value when applied to exceptionally challenging polymorph problems, this is a highly enabling tool that can be used to define crystallization processes and explore their design space regardless of the complexity of the polymorphic system.

Acknowledgment

We gratefully acknowledge the work of Dr. Phil Pye of Merck & Co., Inc. in the development of the reaction crystallization process. We also thank Dr. Hsien-Hsin Tung for his work and insight on the development of the technology mentioned in this manuscript and Dr. Alex Chen for his physical measurements analysis in support of this work.

Received for review April 19, 2009.

OP900095N